
**Supramolecular Chemistry**
Publication details, including instructions for authors and subscription information:
http://www.informaworld.com/smpp/title~content=t713649759

# Free energy perturbation and MM/PBSA studies on inclusion complexes of some structurally related compounds with β-cyclodextrin

M. I. El-Barghouthi[a]; C. Jaime[b]; R. E. Akielah[a]; N. A. Al-Sakhen[a]; N. A. Masoud[a]; A. A. Issa[a]; A. A. Badwan[c]; M. B. Zughul[d]
[a] Department of Chemistry, The Hashemite University, Zarqa, Jordan [b] Department de Quimica, Universitat Autonoma de Barcelona, Bellatterra, Spain [c] The Jordanian Pharmaceutical Manufacturing Company, Naor, Jordan [d] Department of Chemistry, University of Jordan, Amman, Jordan

**To cite this Article** El-Barghouthi, M. I. , Jaime, C. , Akielah, R. E. , Al-Sakhen, N. A. , Masoud, N. A. , Issa, A. A. , Badwan, A. A. and Zughul, M. B.(2009) 'Free energy perturbation and MM/PBSA studies on inclusion complexes of some structurally related compounds with β-cyclodextrin', Supramolecular Chemistry, 21: 7, 603 — 610
**To link to this Article: DOI:** 10.1080/10610270802613562
**URL:** http://dx.doi.org/10.1080/10610270802613562

*Supramolecular Chemistry*
Vol. 21, No. 7, October–November 2009, 603–610

Taylor & Francis
Taylor & Francis Group

# Free energy perturbation and MM/PBSA studies on inclusion complexes of some structurally related compounds with β-cyclodextrin

M.I. El-Barghouthi[a]*, C. Jaime[b], R.E. Akielah[a], N.A. Al-Sakhen[a], N.A. Masoud[a], A.A. Issa[a], A.A. Badwan[c] and M.B. Zughul[d]

[a]*Department of Chemistry, The Hashemite University, Zarqa, Jordan;* [b]*Department de Quimica, Universitat Autonoma de Barcelona, Bellatterra, Spain;* [c]*The Jordanian Pharmaceutical Manufacturing Company, Naor, Jordan;* [d]*Department of Chemistry, University of Jordan, Amman, Jordan*

(*Received 15 March 2008; final version received 2 November 2008*)

Molecular dynamics (MD) simulations have been conducted to explore time-resolved guest–host interactions involving inclusion complex formation between β-cyclodextrin and organic molecules bearing two peripheral benzene rings in aqueous solution. Moreover, free energy perturbation (FEP) and thermodynamic integration (TI) methods at different simulation times have been employed to estimate the relative free energy of complexation. Also, the less computer-time demanding molecular mechanics/Poisson–Boltzmann surface area (MM/PBSA) method was used to estimate the free energy of complexation based on only 1-ns MD simulation. Results showed that both FEP and TI methods were able to reasonably reproduce the experimental thermodynamic quantities. However, long simulation times (e.g. 15 ns) were needed for benzoin mutating to benzanilide (BAN), while moderately shorter times were sufficient for BAN mutating to phenyl benzoate and for benzilic acid mutating to diphenylacetic acid. The results have been discussed in the light of the differences in the chemical structural and conformational features of the guest molecules. In general, it was apparent that the TI method requires less time for convergence of results than the FEP method. However, the less expensive MM/PBSA method proved capable of producing results that are in agreement with those of the more expensive TI and FEP methods.

**Keywords:** molecular dynamics; free energy perturbation; MM/PBSA; cyclodextrin



## Introduction

Natural cyclodextrins (CDs) are a family of macrocyclic oligosaccharides consisting of six (α-CD), seven (β-CD) or eight (γ-CD) α-(1–4)-linked D(+)-glucopyranose units, which are linked in a macrocyclic ring and shaped like truncated cones having hydrophobic hollow cylindrical cavities (*1*). CDs can form inclusion complexes in aqueous solution with a wide variety of organic compounds. They are well known for their ability to increase aqueous solubility, stability and bioavailability of many lipophilic drugs (*1–9*).

Molecular dynamics (MD) provides dynamic and atomic insights to help understand complicated biological systems. Free energy calculation methods have become powerful tools in providing quantitative estimates of guest–host interactions. The most rigorous approaches used to evaluate binding free energies are free energy perturbation (FEP) and thermodynamic integration (TI) methods (*10–12*). However, these methods are computationally expensive. A relatively new method, molecular mechanics/Poisson–Boltzmann surface area (MM/PBSA), was proposed in the past few years for evaluating the binding free energies of macromolecules and their complexes (*13–23*). As the TI and FEP runs required significantly longer simulation runs to converge the free energy estimates, the MM–PBSA is an efficient alternative.

The purpose of the present work was to study the interactions between some closely related organic molecules (Scheme 1) and β-CD that are responsible for complex formation using MD simulations. The two methodologies (FEP and TI) in addition to MM/PBSA were applied to calculate the relative Gibbs free energy of complexation. The effect of the simulation run time on the quality of the FEP and TI output results was also examined.

The guest molecules were chosen based on the following criteria: the molecules have similar components (two peripheral benzene rings) separated by connecting bridges having slightly different functionalities with respect to guest/β-CD interactions (slightly different dimensions, 3D structures and flexibility), forming the same type of guest–host complexes in aqueous solutions (1:1 molar ratio) and availability of rigorously estimated experimental values of complexation free energies. It would therefore be interesting to compare the capability of the three computational techniques (FEP, TI and the

*Corresponding author. Email: musab@hu.edu.jo

ISSN 1061-0278 print/ISSN 1029-0478 online

DOI: 10.1080/10610270802613562
http://www.informaworld.com

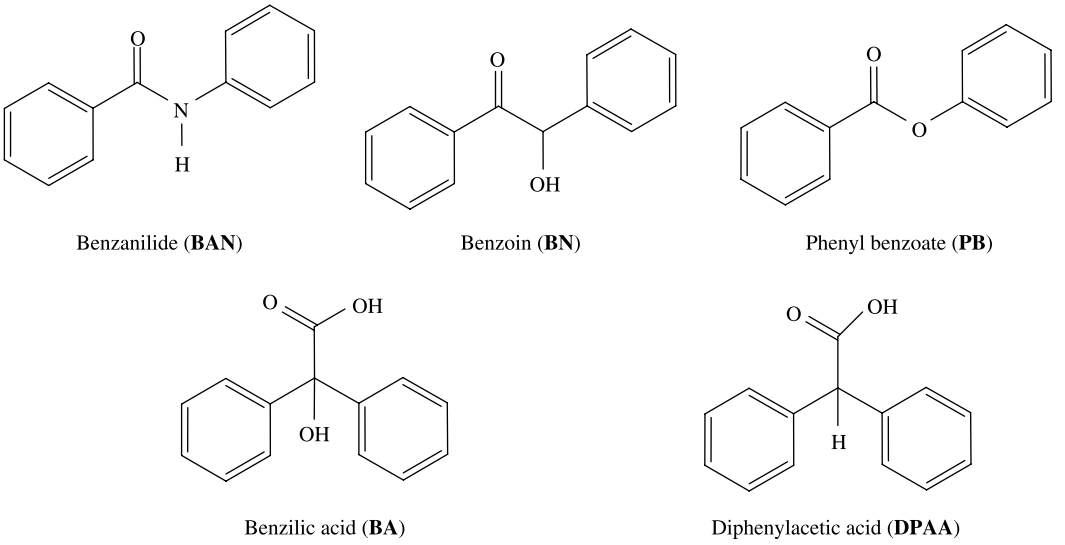


Scheme 1. Structures of the studied guest compounds.



relatively computational cost-effective MM/PBSA) to predict reasonable complexation binding free energies.

## Results and discussion

Phase solubility diagrams (PSDs) for the neutral guest molecules were carried out according to Higuchi and Connors (*24*). The solubility of each guest against β-CD concentration was measured in 0.1 M phosphate buffer at 25°C [pH 6.0 for benzanilide (BAN), phenyl benzoate (PB) and benzoin (BN), whereas pH 1.0 for benzilic acid (BA) and diphenylacetic acid (DPAA)]. Analysis of the whole PSDs to estimate the complex formation constant of the appropriate complex stoichiometry was carried out using rigorous procedures discussed elsewhere (*25, 26*). Detailed discussion of the results can be found in a report published in the proceedings of the 12th International Cyclodextrin Symposium (*27*). Here, a summary of the main results will be presented. BAN, BN, BA and DPAA exhibit $A_L$-type PSDs indicating the formation of soluble complexes, while PB exhibits $B_S$ type. Table 1 lists the corresponding complexation parameters obtained through rigorous analysis of the whole PSDs indicating that all guest molecules form 1:1-type complexes with β-CD.

Table 1. Estimates of the guest/β-CD complexation parameters obtained from rigorous analysis of the PSDs obtained at 25°C.

| Compound | $S_o$ (mM) | $K_{11}$ ($M^{-1}$) | $\Delta G$ (kJ/mol) | PSD type |
|---|---|---|---|---|
| BAN | 0.078 | 121 | −11.89 | $A_L$ |
| PB | 0.059 | 2141 | −19.01 | $B_s$ |
| BN | 0.122 | 1074 | −17.3 | $A_L$ |
| BA | 4.687 | 747 | −16.4 | $A_L$ |
| DPAA | 0.299 | 3453 | −20.19 | $A_L$ |

### *Computational results*

Two orientations of the BN, BAN and PB guests (Scheme 1) within the β-CD cavity were considered: where the benzoyl group is located near the narrow rim of β-CD (A orientation) and the remaining part of the guest is located near the narrow rim (B orientation; as an example see Figure 1). For DPAA and BA molecules, only one starting orientation was considered.

The average structures of the corresponding 1:1 complexes have been calculated for both A and B orientations (if applicable) and are shown in Figure 2.

The average structure of BN/β-CD for orientation A involves the penetration of the benzoyl group into the β-CD cavity, where the carbonyl and hydroxyl groups interact with the secondary hydroxyl group network at the wide rim of the β-CD cavity, leaving the phenyl ring just protruding outside. The corresponding average structure for orientation B appears almost exactly the opposite of orientation A. Unlike BN/β-CD, where both the carbonyl and hydroxyl groups interact with the secondary hydroxyls of β-CD, the average structure of BAN/β-CD shows that the amide group is deeply embedded within the β-CD cavity near the narrow rim, and is more favourably interacting with the glucoside ether linkages, in both orientations A and B. There is however a great deal of distortion in orientation B, where the secondary hydroxyl network becomes more compact (more drawn towards the benzoyl phenyl group), while the primary network becomes scattered over a wider range away from the anilide phenyl group. An almost similar situation is observed for orientation A of the average structures of PB/β-CD and BAN/β-CD, where the ester group of PB favourably interacts with the glucoside ether linkages deep within the β-CD cavity, leaving the two peripheral

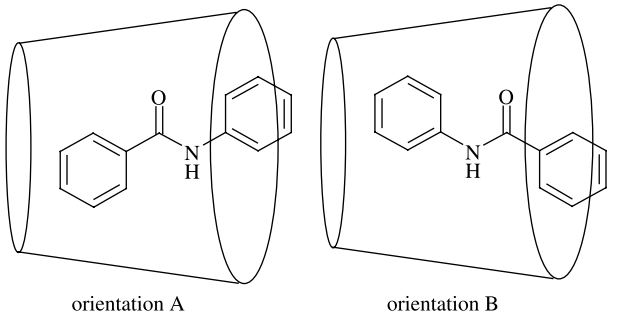


Figure 1. The two orientations of the BAN/β-CD inclusion complex.

phenyl rings each opposite to the hydroxyl group network on either side of the cavity. By contrast, the benzoyl group in orientation B is deeply embedded within the β-CD cavity. The average structures of BA/β-CD and DPAA/β-CD are almost identical where, in both cases, the carboxyl group is favourably interacting with the secondary hydroxyl group network at the wide rim, one phenyl group is just outside the wide rim, whereas the other phenyl group is deeply embedded within the β-CD cavity. In BA/β-CD, the hydroxyl group of BA is similarly hydrogen bonded to the secondary hydroxyl group network.

### *MM/PBSA method*

Table 2 lists the binding free energies (kJ/mol) obtained from the MM/PBSA computational analysis of the β-CD complexes and their corresponding components.

The results listed in Table 2 indicate that the contribution of van der Waals interactions to the total interaction energy is much larger than electrostatic interactions for all studied complexes. $\Delta G_{NP}$ values are negative for all studied complexes indicating that the apolar surface term contributes positively to complex stability, though to a much lower extent compared with van der Waals interactions. Moreover, Table 2 indicates unfavourable electrostatic solvation energy (positive $\Delta G_{PB}$) resulting in an overall positive value of the solvation free energy ($\Delta G_{solv} = \Delta G_{PB} + \Delta G_{NP}$). Therefore, it is safe to conclude that the apolar components ($\Delta G_{apolar} = \Delta E_{vdW} + \Delta G_{NP}$)

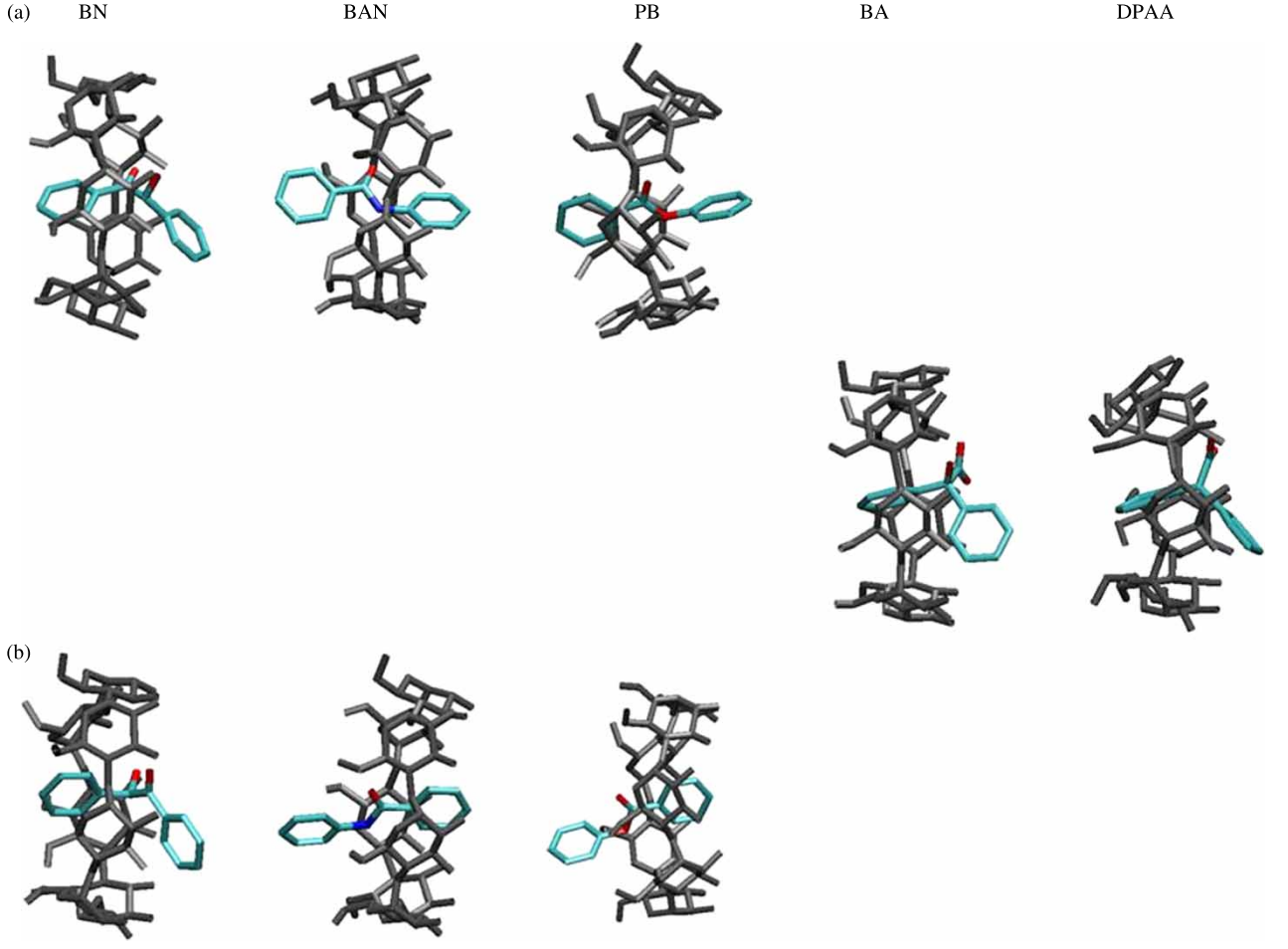


Figure 2. Average structures of the guest/β-CD inclusion complexes: (a) orientation A and (b) orientation B.

Table 2. Binding free energies and their corresponding components (kJ/mol) obtained from MM/PBSA computational analysis of the β-CD complexes with BAN, PB, BN, BA and DPAA.

| | Orientation | $\Delta E_{elect}$ | $\Delta E_{vdW}$ | $\Delta G_{NP}$ | $\Delta G_{PB}$ | $\Delta G_{polar}$ | $\Delta G_{apolar}$ | $\Delta G^{a}$ | $-T\Delta S$ | $\Delta G$ |
|---|---|---|---|---|---|---|---|---|---|---|
| BAN | A | −17.39 | −100.19 | −9.61 | 73.86 | 56.47 | −109.80 | −53.33 | 64.08 | 10.75 |
| | B | −7.69 | −99.32 | −9.82 | 66.00 | 58.31 | −109.14 | −50.83 | 62.53 | 11.70 |
| PB | A | −14.88 | −106.46 | −9.99 | 70.35 | 55.47 | −116.45 | −60.98 | 64.75 | 3.77 |
| | B | −5.68 | −99.32 | −9.57 | 48.32 | 42.64 | −108.89 | −66.25 | 61.40 | −4.85 |
| BN | A | −17.01 | −106.34 | −10.20 | 76.33 | 59.32 | −116.54 | −57.22 | 65.42 | 8.20 |
| | B | −20.57 | −107.55 | −10.20 | 78.00 | 57.43 | −117.75 | −60.32 | 67.76 | 7.44 |
| BA | – | −22.78 | −115.12 | −10.49 | 81.68 | 58.90 | −125.61 | −66.71 | 72.90 | 6.19 |
| DPAA | – | −21.44 | −113.70 | −10.53 | 76.95 | 55.51 | −124.23 | −68.72 | 70.77 | 2.05 |

$\Delta G_{polar} = \Delta E_{elect} + \Delta G_{PB}$.

$\Delta G_{apolar} = \Delta E_{vdW} + \Delta G_{NP}$.

$\Delta G^{a} = \Delta E_{vdW} + \Delta E_{elect} + \Delta G_{NP} + \Delta G_{PB}$.

$\Delta G = \Delta G^{a} - T\Delta S$.

contribute positively to the binding free energies, while the overall electrostatic term contributes negatively to the complex formation. However, the differences in the binding free energies for the studied molecules could not be accounted for only by the apolar term without the polar term since the values of both terms span ≈17 kJ/mol.

It is also worth noting that the $\Delta G_{PB}$ value for orientation B of the PB/β-CD complex is much lower than those predicted for all other guest complexes (the least positive value). Returning to the obtained average structures (Figure 2) reveals that for the PB molecule in the B orientation of the PB/β-CD complex, the benzoyl group is included whereas the phenoxy group protrudes to interact with bulk water. Since the MM/PBSA methodology utilises the continuum salvation model that ignores solute–solvent-specific interactions, this explains the unusual difference observed in the $\Delta G_{PB}$ value from those of other guests.

Moreover, the results also show that orientation B is more favoured than orientation A for BN and PB, whereas orientation A is favoured for BAN. However, in both the BN/β-CD and BAN/β-CD complexes, the difference between orientations A and B is $< 1$ kJ/mol, thus suggesting the possible formation of isomeric complexes at 298 K.

NMODE calculations indicate that in both types of complexes, negative $\Delta S_{conf}$ values were obtained for all studied compounds (Table 2) thus indicating a reduction of guest and host configurational freedom upon complexation. However, NMODE calculations overestimate the rotational/translational entropy loss upon binding.

### *FEP techniques*

Both FEP and TI methodologies were applied to calculate the relative differences in the binding free energies of BN, BAN, PB, BA and DPAA complexing with β-CD in water. The thermodynamic cycle relevant to this study is shown in Figure 3. Two FEPs/TIs were considered to close the thermodynamic cycle, for the mutation of solvated guest: (1) to solvated guest (2) before and after complexation.

### *Free energy perturbation*

Both forward and reverse runs were conducted and the resulting $\Delta\Delta G$ values were averaged. The $\Delta\Delta G_{comp}$ (kJ/mol) results of the simulations performed for the mutations of BAN → PB, BN → BAN and BA → DPAA together with the corresponding experimental data are listed in Table 3. The results in Table 3 show that the values of $\Delta\Delta G_{comp}$ calculated in the forward and reverse directions were fairly close in magnitude, thus exhibiting very low hysteresis. However, this low hysteresis does not necessarily imply accuracy of the obtained results that showed great dependence on simulation run time as is discussed later.

The experimental data (*24*) reveal that BN has a higher tendency to form a complex with β-CD than BAN by 5.4 kJ/mol. Also, the PB complex is more stable than the BAN complex by 7.1 kJ/mol. In addition, the DPAA complex is more stable than the BA complex by 3.8 kJ/mol. Generally speaking, the FEP method predicts the same trend observed experimentally regardless of orientation.

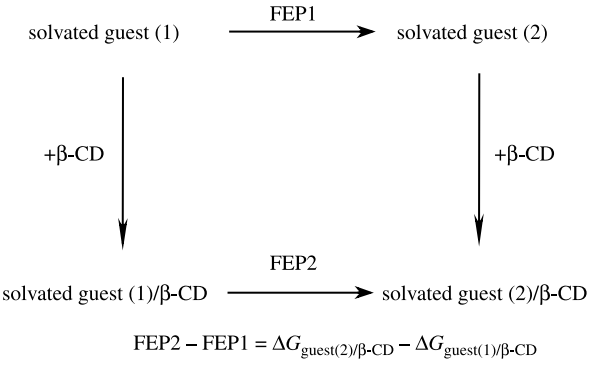


Figure 3. Thermodynamic cycle used to computationally evaluate the free energy differences.

Table 3. The relative binding free energies $\Delta\Delta G_{comp}$ (kJ/mol) computed using FEP, TI and MM/PBSA techniques applied for BAN → PB, BN → BAN and BA → DPAA mutations.

| | | | FEP | | | TI | | | | |
|---|---|---|---|---|---|---|---|---|---|---|
| Mutation | Orientation | | 5 ns | 10 ns | 15 ns | 5 ns | 10 ns | 15 ns | MM/PBSA | $\Delta\Delta G_{expt}$ |
| BAN → PB | A | Forward | −4.40 | −5.32 | −4.90 | | | | | −7.12 |
| | | Reverse | 4.34 | 5.34 | 4.89 | −4.01 | −4.38 | −5.29 | −6.98 | |
| | | Average | −4.37 | −5.33 | −4.90 | | | | | |
| | B | Forward | −4.89 | −5.03 | −4.81 | | | | | |
| | | Reverse | 4.94 | 5.08 | 4.83 | −4.44 | −4.66 | −5.22 | −16.55 | |
| | | Average | −4.92 | −5.06 | −4.82 | | | | | |
| BN → BAN | A | Forward | 15.97 | 0.21 | 3.85 | | | | | 5.41 |
| | | Reverse | −15.44 | −0.20 | −3.41 | 8.17 | 4.14 | 4.09 | 2.55 | |
| | | Average | 15.71 | 0.21 | 3.63 | | | | | |
| | B | Forward | 4.24 | 3.73 | 2.14 | | | | | |
| | | Reverse | −3.59 | −3.02 | −1.66 | 8.17 | 5.70 | 7.16 | 4.26 | |
| | | Average | 3.92 | 3.38 | 1.90 | | | | | |
| BA → DPAA | – | Forward | 0.72 | 0.06 | −0.52 | | | | | −3.79 |
| | | Reverse | −0.67 | 0.00 | 0.55 | −0.55 | −0.19 | −0.36 | −4.14 | |
| | | Average | 0.70 | 0.03 | −0.54 | | | | | |

Also, for BAN → PB mutation, the theoretical results obtained using FEP were close to experimental data. Moreover, the results of different time simulations were close indicating free energy convergence. This was not the case for BN → BAN mutation, which means that long simulation times were needed for BN mutating to BAN, while relatively shorter times were sufficient for BAN to mutate to PB. This may be explained by the fact that the difference in chemical and conformational structures between BN and BAN (C—OH vs. N—H groups) is more pronounced than for BAN and PB (N—H vs. O groups). BN has a non-coplanar structure whereas BAN assumes a planar structure due to the partial double bond character of the C—N amide linkage (look up the average complex structures in Figure 2). Therefore, more time is needed here to reproduce the conformational changes.

For the BA → DPAA mutation, the theoretical results indicate that FEP was able to predict the experimental sign. Moreover, the results of different time simulations showed fewer fluctuations than that in BN → BAN mutation. This can be explained by noting that the average complex structures of BA and DPAA with β-CD obtained by the MD simulations were more or less the same.

To investigate that point further, the individual free energy contributions to the total $\Delta\Delta G_{comp}$ value for approach A (when applicable) are listed in Table 4.

Table 4. Individual FEP energy term contributions as a function of simulation time for approach A (when applicable).

| | FEP2–FEP1 (5 ns) | FEP2–FEP1 (10 ns) | FEP2–FEP1 (15 ns) |
|---|---|---|---|
| BN → BAN (COH → NH) | | | |
| Electrostatic | −2.57 | −13.49 | −9.22 |
| 1–4 Electrostatic | −8.80 | 1.54 | −1.52 |
| Non-bonded | 13.84 | 11.31 | 10.19 |
| 1–4 Non-bonded | 1.15 | −0.48 | 0.33 |
| BADH | 12.07 | 1.14 | 3.84 |
| BAN → PB (NH → O) | | | |
| Electrostatic | −5.73 | −7.03 | −6.32 |
| 1–4 Electrostatic | −0.08 | −0.11 | −0.05 |
| Non-bonded | 1.14 | 1.32 | 1.24 |
| 1–4 Non-bonded | −0.03 | −0.05 | −0.04 |
| BADH | 0.39 | 0.54 | 0.28 |
| BA → DPAA (OH → H) | | | |
| Electrostatic | 7.54 | 2.45 | 5.98 |
| 1–4 Electrostatic | −7.51 | −3.65 | −6.36 |
| Non-bonded | 4.41 | 3.86 | 3.56 |
| 1–4 Non-bonded | −3.17 | −2.02 | −3.19 |
| BADH | −0.57 | −0.61 | −0.53 |

For BN → BAN mutation, the results in Table 4 show relatively large variations as a function of time, especially for the electrostatic and bond–angle–dihedral (BADH) terms. This confirms what was mentioned above that the guest and host conformations and their relative orientations in this case need more time to evolve. By contrast, for the BAN → PB mutation, each energy contribution changes slightly with time thus indicating convergence. Furthermore, the contribution of the BADH term is $< 0.5$ kJ/mol compared with the larger values of BN → BAN mutation. This explains why a moderate period of time is required for the BAN → PB mutation since little conformational changes take place. The larger variation in the electrostatic term for BN → BAN mutation with time may therefore be attributed to the more exacting COH → NH mutation, which demands more time for the electrostatic contribution to converge.

For the BA → DPAA mutation, the different energy contributions were fairly stable with time except for the electrostatic contribution, which involves an OH → H mutation thus accounting for the observed fluctuations with time.

Table 5. Individual TI energy term contributions as a function of simulation time.

| | TI1 – TI2 (5 ns) | TI1 – TI2 (10 ns) | TI1 – TI2 (15 ns) |
|---|---|---|---|
| BN → BAN (COH → NH) | | | |
| Electrostatic | 1.17 | − 11.64 | − 10.92 |
| 1–4 Electrostatic | − 9.73 | − 3.03 | − 0.53 |
| Non-bonded | 10.33 | 14.92 | 14.36 |
| 1–4 Non-bonded | − 0.74 | 0.25 | − 2.16 |
| BADH | 7.14 | 3.64 | 3.34 |
| BAN → PB (NH → O) | | | |
| Electrostatic | − 5.78 | − 5.87 | − 6.82 |
| 1–4 Electrostatic | − 0.16 | − 0.07 | − 0.05 |
| Non-bonded | 1.28 | 1.22 | 1.30 |
| 1–4 Non-bonded | − 0.03 | − 0.04 | − 0.05 |
| BADH | 0.68 | 0.39 | 0.32 |
| BA → DPAA (OH → H) | | | |
| Electrostatic | 5.97 | 6.59 | 6.34 |
| 1–4 Electrostatic | − 6.63 | − 6.53 | − 6.74 |
| Non-bonded | 4.02 | 3.62 | 3.90 |
| 1–4 Non-bonded | − 3.32 | − 3.28 | − 3.34 |
| BADH | − 0.60 | − 0.59 | − 0.52 |

### *Thermodynamic integration*

The $\Delta\Delta G_{comp}$ (kJ/mol) results of the TI simulations performed for the forward mutations of BN → BAN, BAN → PB and BA → DPAA are listed in Table 3, which shows the calculated $\Delta\Delta G_{comp}$ in the forward direction.

It is obvious that the results obtained by the TI method are in good agreement with experimental data. Moreover, it seems that TI requires less simulation time for convergence. For example, the BN → BAN mutation needs only 10 ns to converge compared with 15 ns in the FEP case. This is shown more clearly by comparing the individual free energy contributions to the total $\Delta\Delta G_{comp}$ for approach A (Table 5). A clear improvement in BN → BAN mutation, especially in the BADH term for orientation A is apparent. Furthermore, general improvements are observed in the results of BAN → PB and BA → DPAA mutations.

### *Comparison between FEP, TI and MM/PBSA methods*

The results in Table 3 indicate that the three methods predict similar trends in the complexation affinities to what was experimentally observed, regardless of orientation. Moreover, the values estimated by the three methods are in a relatively good agreement keeping in mind that long simulation time was required for FEP and TI methods, whereas only 1-ns MD simulation was used for MM/PBSA method. Moreover, the results in Table 3 indicate that even longer simulation runs might be required for FEP to converge, especially for BN → BAN mutation. FEP and TI predict lower relative values of the binding energy for DPAA and BA than the experimental values, while those of MM/PBSA were in excellent agreement with the experimental values. Nevertheless, MM/PBSA overestimates the magnitude of $\Delta\Delta G$ in the case of BAN → PB (orientation B), which is due to the fact that MM/PBSA utilises the continuum solvation model that ignores specific solute–solvent interactions. This apparently leads to the more significant difference between orientations A and B free energies for PB (Table 2, especially the value of $\Delta G_{PB}$) as discussed before. Briefly stated, orientation A leads to complete inclusion of PB into the β-CD cavity, while the phenoxy group of PB remains clearly exposed to the solvent in orientation B. Therefore, the MM/PBSA method yields an overestimate for the magnitude of the binding free energy for the orientation B of PB/β-CD complex, and hence a larger difference in the values observed between those of the B approaches for BAN and PB.

## Conclusions

FEP and TI techniques in addition to the MM/PBSA methodology were conducted to estimate the relative complexation free energies of the closely related organic molecules (BN, BAN, PB, BA and DPAA) with β-CD. In general, the results were in good agreement with the experiment. It was observed that long simulation times were required for FEP and TI simulations involving mutations between two guests that differ highly in their conformational structure such as BN and BAN. However,

the TI method requires less time than FEP calculations. Moreover, the MM/PBSA method appears capable of producing results that are in agreement with those of the more expensive TI and FEP methods.

### *Computational methods*

The initial molecular geometry of β-CD was obtained using X-ray diffraction data (*28*), whereas the starting geometries of the guest molecules were built up from standard bond lengths and bond angles. The AMBER 8 program was used throughout this work (*29*) using Param99 and the general force field parameters sets (*30*). Electrostatic potentials of the studied molecules were computed using *ab initio* HF/6-31G* calculations through the Gaussian 03W package (*31*). Atomic charges reproducing these electrostatic potentials were obtained using the RESP methodology (*32*); the RESP charges used for all molecules involved in this study are given in the attached Supplementary material.

All molecules were solvated by a cubic box of TIP3P water molecules (*33*) with a closeness parameter of 9 Å away from the boundary of any CD or guest atoms. Periodic boundary conditions were adopted and the particle mesh Ewald method was used for the treatment of long range electrostatic interactions (*34*). The non-bonded cut-off was set to 8.0 Å and the SHAKE option was used to constrain the bonds involving hydrogen atoms (*35*).

Energy minimisation was performed for each solvated complex using the conjugate gradient algorithm, heated up to 298 K for 50 ps. Another 50-ps simulation at 298 K and constant volume was conducted, followed by 200 ps more for achieving equilibration at 298 K and 1 atm. Production runs were carried out for 1000 ps; the system was coupled in the NPT ensemble to a Berendsen thermostat at 298 K and a barostat at 1 atm. A 1-fs time step with a saving of the structure every 1 ps was used and the non-bonded pair list was updated every 25 steps.

Analysis of the obtained MD trajectories (hydrogen bonds and average structures) was conducted using the PTRAJ module of AMBER.

FEP and TI methods were carried out by window methods. Each mutation was conducted in 101 (FEP) or 21 (TI) windows using $\Delta\lambda$ of 0.01 (FEP) or 0.05 (TI). Different simulation times were used ranging from 5 up to 15 ns. Equilibration was conducted for 40% of the specified time and data were collected for the remaining 60% at each window.

For the MM–PBSA methodology, snapshots were taken at 1-ps intervals from the corresponding 1000-ps MD trajectories. Snapshots of the unbound guest and β-CD molecules were also taken from the corresponding guest/β-CD trajectories. The energy components were calculated using very large cut-off (999 Å).

The explicit water molecules were removed from the snapshots. The binding free energy, $\Delta G_{\text{bind}}$, was estimated as follows:

$$\Delta G_{\text{bind}} = \Delta E_{\text{gas}} + \Delta G_{\text{solv}} - T\Delta S_{\text{conf}}, \quad (1)$$

where $\Delta E_{\text{gas}}$ is the interaction energy between the guest and β-CD in the gas phase, which is given by

$$\Delta E_{\text{gas}} = \Delta E_{\text{elect}} + \Delta E_{\text{vdW}}, \quad (2)$$

where $\Delta E_{\text{elect}}$ and $\Delta E_{\text{vdW}}$ represent the guest–host electrostatic and van der Waals interactions, respectively.

The solvation free energy ($\Delta G_{\text{solv}}$) was estimated as the sum of electrostatic solvation free energy ($\Delta G_{\text{PB}}$) and apolar solvation free energy ($\Delta G_{\text{NP}}$):

$$\Delta G_{\text{solv}} = \Delta G_{\text{PB}} + \Delta G_{\text{NP}}. \quad (3)$$

$\Delta G_{\text{PB}}$ was computed for continuum solvent using the PBSA program of AMBER 8 (*19*), while $\Delta G_{\text{NP}}$ was calculated from the solvent-accessible surface area (SASA). A probe radius of 0.14 nm and atomic radii of the PARSE parameter set (*36*) were used to determine the molecular surface. The MSMS program (*37*) was used to calculate the SASA required for the estimation $\Delta G_{\text{NP}}$ given by

$$\Delta G_{\text{NP}} = \gamma \cdot \text{SASA} + b, \quad (4)$$

where $\gamma = 0.00542$ kcal/(mol Å$^2$) and $b = 0.92$ kcal/mol.

The change of solute entropy upon complexation, $T\Delta S_{\text{conf}}$, was estimated from normal mode analysis using the NMODE module of the AMBER 8 program. A distance-dependent dielectric function $\varepsilon = 4r_i$ was used, and a convergence criterion of 0.0001 kcal/mol was set for the energy gradient.

## Acknowledgements

The authors wish to thank the Hashemite University and The Jordanian Pharmaceutical Manufacturing Company (JPM) for their financial support.

## References

(1) Duchene, D. *Cyclodextrins and their Industrial Uses*; Editions de Santé: Paris, 1987.
(2) Szejtli, J. *Chem. Rev.* **1998**, *98*, 1743–1754.
(3) Uekama, K.; Hirayama, F.; Irie, T. *Chem. Rev.* **1998**, *98*, 2045–2076.
(4) Omar, L.; El-Barghouthi, M.I.; Masoud, N.; Abdoh, A.A.; Al Omari, M.; Zughul, M.B.; Badwan, A.A. *J. Soln Chem.* **2007**, *36*, 605–616.
(5) El-Barghouthi, M.I.; Masoud, N.; Al-Kafawein, J.; Zughul, M.B.; Badwan, A.A. *J. Incl. Phenom. Macro. Chem.* **2005**, *53*, 15–22.
(6) Harada, A. *Acc. Chem. Res.* **2001**, *34*, 456–464.

(7) Pose-Vilarnovo, B.; Perdomo-Lopez, I.; Echezarreta-Lopez, M.; Schroth-Padro, P.; Estrada, E.; Tores-Labandeira, J.J. *Eur. J. Pharm. Sci.* **2001**, *13*, 325–331.
(8) Loftsson, T.; Duchene, D. *Int. J. Pharm.* **2007**, *329*, 1–11.
(9) Szente, L.; Szejtli, J. *Trends Food Sci. Technol.* **2004**, *15*, 137–142.
(10) Kollman, P.A. *Chem. Rev.* **1993**, *93*, 2395–2417.
(11) Kollman, P.A.; Cieplak, P. *J. Comput. Aided Mol. Des.* **1993**, *7*, 291–304.
(12) Mark, A.E.; van Helden, S.P.; Smith, P.E.; Janssen, L.H.M.; van Gunsteren, W.F. *J. Am. Chem. Soc.* **1994**, *116*, 6293–6302.
(13) Srinavasan, J.; Cheatham, T.E.; Cieplak, P.; Kollman, P.A.; Case, D.A. *J. Am. Chem. Soc.* **1998**, *120*, 9401–9409.
(14) Fogolari, F.; Tosatto, S.C.E. *Protein Sci.* **2005**, *14*, 889–901.
(15) Gohlke, H.; Case, D.A. *J. Comput. Chem.* **2004**, *25*, 238–250.
(16) Kuhn, B.; Gerber, P.; Schulz-Gasch, T.; Stahl, M. *J. Med. Chem.* **2005**, *48*, 4040–4048.
(17) Kuhn, B.; Kollman, P.A. *J. Med. Chem.* **2000**, *43*, 3786–3791.
(18) Lee, M.R.; Duan, Y.; Kollman, P.A. *Proteins: Struct. Funct., Genet.* **2000**, *39*, 309–316.
(19) Wang, J.; Morin, P.; Wang, W.; Kollman, P.A. *J. Am. Chem. Soc.* **2001**, *123*, 5221–5230.
(20) Wang, W.; Kollman, P.A. *J. Mol. Biol.* **2000**, *303*, 567–582.
(21) Pearlman, D.A. *J. Med. Chem.* **2005**, *48*, 7796–7807.
(22) Lyne, P.D.; Lamb, M.L.; Saeh, J.C. *J. Med. Chem.* **2006**, *49*, 4805–4808.
(23) Weis, A.; Katebzadeh, K.; Soderhjelm, P.; Nilsson, I.; Ryde, U. *J. Med. Chem.* **2006**, *49*, 6596–6606.
(24) Higuchi, T.; Connors, K.A. *Adv. Anal. Chem. Instrum.* **1965**, *4*, 117–212.
(25) Zughul, M.B.; Badwan, A.A. *Int. J. Pharm.* **1997**, *151*, 109–119.
(26) Zughul, M.B.; Badwan, A.A. *J. Incl. Phenom. Mol. Recog. Chem.* **1998**, *31*, 243–264.
(27) El-Barghouthi, M.I.; Al-Souod, K.A.; Zughul, M.B.; Badwan, A.A. *Proceedings of the 12th International Cyclodextrin Symposium*, Montpellier, France, 16–19 May, 2004, pp 267–270.
(28) Linder, K.; Saenger, W. *Carbohyd. Res.* **1982**, *99*, 103–115.
(29) Case, D.A.; Darden, T.A.; Cheatham, T.E.; Simmerling, C.L.; Wang, J.; Duke, R.E.; Luo, R.; Merz, K.M.; Wang, B.; Pearlman, D.A.; Crowley, M.; Brozell, S.; Tsui, V.; Gohlke, H.; Mongan, J.; Hornak, V.; Cui, G.; Beroza, P.; Schafmeister, C.; Caldwell, J.W.; Ross, W.S.; Kollman, P.A. AMBER 8, University of California, San Francisco, CA, 2004.
(30) Cornell, W.D.; Cieplak, P.; Bayly, C.I.; Gould, I.R.; Merz, K.M., Jr.; Ferguson, D.M.; Spellmeyer, D.C.; Fox, T.; Caldwell, J.W.; Kollman, P.A. *J. Am. Chem. Soc.* **1995**, *117*, 5179–5197.
(31) Frisch, M.; Trucks, G.; Schlegel, H.; Scuseria, G.; Robb, M.; Cheeseman, J.; Montgomery, J.; Vreven, Jr.; Kudin, K.; Burant, J.; Millam, J.; Iyengar, S.; Tomasi, J.; Barone, V.; Mennucci, B.; Cossi, M.; Scalmani, G.; Rega, N.; Petersson, G.; Nakatsuji, H.; Hada, M.; Ehara, M.; Toyota, K.; Fukuda, R.; Hasegawa, J.; Ishida, M.; Nakajima, T.; Honda, Y.; Kitao, O.; Nakai, H.; Klene, M.; Li, X.; Knox, J.; Hratchian, H.; Cross, J.; Adamo, C.; Jaramillo, J.; Gomperts, R.; Stratmann, R.; Yazyev, O.; Austin, A.; Cammi, R.; Pomelli, C.; Ochterski, J.; Ayala, P.; Morokuma, K.; Voth, G.; Salvador, P.; Dannenberg, J.; Zakrzewski, V.; Dapprich, S.; Daniels, A.; Strain, M.; Farkas, O.; Malick, D.; Rabuck, A.; Raghavachari, K.; Foresman, J.; Ortiz, J.; Cui, Q.; Baboul, A.; Clifford, S.; Cioslowski, J.; Stefanov, B.; Liu, G.; Liashenko, A.; Piskorz, P.; Komaromi, I.; Martin, R.; Fox, D.; Keith, T.; Al-Laham, M.; Peng, C.; Nanayakkara, A.; Challacombe, M.; Gill, P.; Johnson, B.; Chen, W.; Wong, M.; Gonzalez, C.; Pople, J. *Gaussian 03, Revision A.1*; Gaussian, Inc., Pittsburgh, PA, 2003.
(32) Bayly, C.I.; Cieplak, P.; Cornell, W.D.; Kollman, P.A. *J. Phys. Chem.* **1993**, *97*, 10269–10280.
(33) Jorgensen, W.L.; Chandrasekhar, J.; Madura, J.D.; Impey, R.W.; Klein, M.L. *J. Chem. Phys.* **1983**, *79*, 926–935.
(34) Darden, T.; York, D.; Pedersen, L. *J. Chem. Phys.* **1993**, *98*, 10089–10092.
(35) van Gunsteren, W.F.; Berendsen, H.J.C. *Mol. Phys.* **1977**, *34*, 1311–1327.
(36) Stikoff, D.; Sharp, K.A.; Honig, B. *J. Phys. Chem.* **1994**, *98*, 1978–1988.
(37) Sanner, M.F.; Olson, A.J.; Spehner, J.C. *Biopolymer* **1996**, *38*, 305–320.